McNair Research Journal SJSU

Volume 15 *Spring 2019* Article 11

2019

Investigation into the Effects of Blade Tip Twist on Noise Reduction for a NACA 0012 Rotor Blade

Uyen T. Sou
San Jose State University

Uyen T. Sou

Major:
Aerospace Engineering

Mentor:
Dr. Nicholas B. Cramer, **Dr. Sean Swei**

Investigation into the Effects of Blade Tip Twist on Noise Reduction for a NACA 0012 Rotor Blade

Biography

Uyen aspires to integrate her passion for learning, aerospace, and art to impact the world around her in a positive way. She is inspired by her family, advisors, and friends around her that give her the confidence to pursue her goals. She is also inspired by the professors and mentors who have helped and continue to help broaden her mind every day. Being a first-generation student has proven to be a challenge as well as a driving force that motivates her to give it her all and try out things she thought she never could. She hopes to make an impact in industry and become a professor in her field in the future. She was involved with Rocket Club earning a level 1 certification from Tripoli Rocketry Association and is a member of the American Institute of Aeronautics and Astronautics. She is also involved with community outreach programs that encourage the next generation of engineers such as the Engineering Ambassadors Program as well as Project Lead the Way here at San José State University.

Investigation into the Effects of Blade Tip Twist on Noise Reduction for a NACA 0012 Rotor Blade

ABSTRACT

The advancement of the urban air mobility concept is heavily dependent on the public acceptance of the aircraft vehicles used for air taxis. The importance of the perception of noise by humans is crucial to the passing of legislation and proposals working to implement the new transport system. The investigation into how the noise perception can be reduced is vital to the success of the personal air travel industry. The air taxi design has been geared towards the rotorcraft models. Therefore, the investigation into the rotor blade designs is necessary because, similar to helicopters, the main component in noise generation is the rotors and its blades. The blade-vortex interaction creates noise which humans perceive as the most annoying and disruptive type of noise produced by rotorcraft. The blade-vortex interaction noise is due to the interaction between the advancing blade and the vortexes generated by the tips of the previous rotor blade. This study looks into the effect of tip twist on rotor blades. Understanding how twist in a blade will affect thrust production and noise production will aid in the progress of developing the acceptance of the urban air mobility movement. This investigation is carried out through the use of high-fidelity rotorcraft modeling software developed by Continuum Dynamics Incorporated called the Comprehensive Hierarchical Aeromechanics Rotorcraft Model (CHARM) coupled with the aeroacoustic processing package PSU-WOPWOP to produce sound data files at the wake of the rotor blades. The noise reducing parameter under investigation is the tip twist of the rotor blades. Particularly, interest is on how this change affects the frequency of sound pressure levels. The reduction of this type of noise will aid in determining the design of efficient and safe air taxis that will utilize a system of smaller porting stations as drop off zones, similar, only in concept, to those ride-sharing services.

I. Nomenclature

BVI = blade-vortex interaction
SPL = Sound Pressure Level
dBA = A-weighted decibel, a metric for sound annoyance
dB = decibel, a measure of sound level
BWI = blade-wale interaction noise

II. Introduction

The rise of interest in the Urban Air Mobility has prompted the Federal Aviation Administration to implement requirements and policies about noise restrictions [1]. This means air taxi vehicles must meet noise certification requirements in order to be successfully integrated as a new transportation system [2]. The impacts of air taxis on the community must be considered for successful integration. Such impacts include noise, flight path design, and landing and takeoff zones [1]. Although all the above are integral to the successful integration of air taxis, the impact of noise to communities is the focus of this paper.

The human ear does not linearly relate frequencies in sound to how loud a frequency is. Loudness is defined as the magnitude of the feeling in the human ear due to a change in the air pressure. Human ears are more sensitive to changes in air pressure than they are to constant air pressure meaning noise that frequently changes in pitch is more annoying than a constant noise [3]. In this setting, air pressure is referring to the volume of air that each rotor blade displaces as it rotates. The volume displaced is dependent on the rate at which the blade rotates, amount of pressure the blade absorbs, blade tip velocity, and amount of power used to produce the rotation [4]. The amount of volume displaced and the rate at which the volume is displaced plays into the noise humans hear. The unit of noise annoyance is the A-weighted decibel, dBA. The unit dBA is based off of a logarithmic scale of annoyance [5].The National Aeronautics and Space Administration's (NASA) preliminary fly-over testing of small unmanned air vehicles suggested the tolerance of noise based on the A-weighted sound pressure level to about 65 dBA at 15*m* or 50 *feet* from the source of the noise is an acceptable noise range [6].

Many air taxi designs resemble that of a helicopter therefore, the main source of noise for air taxis is also from its rotors like it is for helicopters [7]. The general noise mechanisms that have been associated with rotors are discrete loading noise, broadband noise, broadband self-noise, and discrete impulsive noise [8, 9]. As defined by Brooks *et al*., the discrete loading noise is caused by the blade loading that occurs at lower steady frequencies [8]. The broadband noise occurs due to the blade interacting with the turbulent flow of the wake, also known as the blade-wake interactions (BWI) [5]. The broadband self-noise is described as the noise produced when the blade comes into contact with the turbulent flow surrounding the rotor wake and the boundary layers formed along the blade [8]. The discrete impulsive noise is the blade loading that occurs predominately at the tips of the rotor blade and is distinguished from discrete loading noise by its impulsive nature. This type of noise is also known as blade-vortex interaction (BVI) noise and can over take other types of noise due to BVI noise occurring at the high frequencies [3, 8]. Past investigations into noise reduction suggest there is significance in attempting to employ noise reduction methods that aim to minimize the noise produced within the same plane of the rotor blade [9]. The methods are broken down into passive and active means of reducing noise. The noise mechanisms found in the rotor blade plane are thickness noise and high-speed impulsive noise [7, 9]. One passive noise reduction method involves reducing the rotational speed of the rotor [9]. Shi *et al*. [9, 10] noted that the reduced speed of the rotor blade, measured in rotations per minute (RPM), was effective in reducing the noise in-plane of the rotor blade. However, passive methods such as reducing the rotational speed of the rotor negatively affects the performance of the rotorcraft because the thrust production is also decreased [9]. This adversely impacts the amount of weight the rotorcraft can carry on board as well as the safety of the rotorcraft due to increased vibrations found at lower rotational speeds [7]. Malovrh *et al*. [10] discussed a few passive methods including adjusting the tip-path-angle by identifying areas of zero inflow experienced by the rotor blade. Rotor noise consists of the blade-vortex interaction, thickness noise, loading noise, and high-speed impulsive noise. The following provides a breakdown of noise types:

- **Blade-Vortex Interaction Noise:** the impulsive loading noise due to tip vortex interference with the following blade [1]
- **Thickness Noise:** the noise produced by the displacement of fluid by the rotor blade [1] • **Loading Noise:** the noise produced by a force exerted onto the fluid by the rotor blade surface [1]

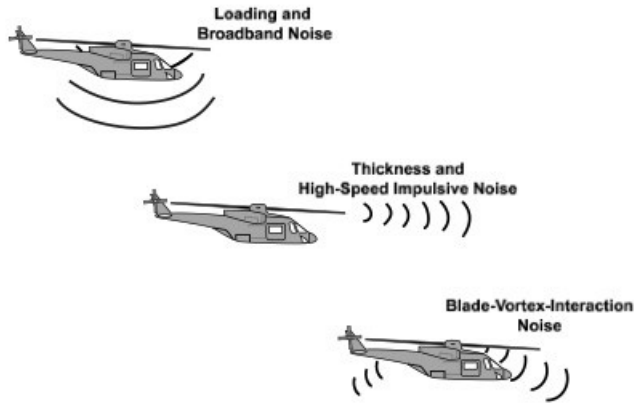

Fig. 1: The three primary rotor noise sources [11].

Blade-vortex interaction (BVI) noise is in the frequency range humans perceive to be the most annoying because of the impulsive nature of BVI noise. BVI noise is generated during low speed descent and during forward flight [7, 10]. These two maneuvers occur often during air taxi operations, so attempts in reducing the production of BVI noise is important in meeting noise restrictions criteria for air taxis. The design mechanisms available to reduce noise is limited for rotorcrafts and must rely on source noise reduction rather than noise control mechanisms [11]. For example, airplane engines have available noise suppression ducts and noise absorbing lining material for their engines that reduces the noise generated by the engine blades. Due to the nature and design of rotorcraft, this is not an option. Source noise reduction can be achieved using passive and active methods of noise reduction. Therefore, most passive attempts to reduce noise leans towards the design of the blade tips in order to gain a balance between noise reduction and overall performance [7, 8].

Malovrh *et al*. [10] provided a detailed overview of the advanced blade tip configurations that had success in decreasing the intensity of the tip vortex such as the Ogee tip described by Landgrebe and Bellinger [12]. These advanced tip configurations look at the effects of sweep, taper, thickness, and anhedral on the blade tip. Yu *et al*. documented many tip configurations suggested to aid in the reduction of BVI noise. The suggested configurations were parabolic, elliptic, bulge, and vane tips [7]. Brocklehurst *et al*. [13] reviewed the Ogee tip that was designed to decrease the intensity of the tip vortex. The results concluded decrease in tip vortex strength help in reducing the noise production because the advancing blade interacting with the vortex will displace air that are of a lesser pressure difference [10]. Another experiment investigated noise reduction of the BERP blade developed through the British Experimental Rotor Programme. The experiment divided the tip vortex into smaller vortices using sweep and anhedral at the blade tip [13]. The results of the experiment concluded no best design of the blade tip has been developed [13]. Active modes of reducing rotor noise are through high harmonic controls (HHC), single blade control, active twist, and active flaps [9]. These active methods are generally used for the reduction of BVI noise but have been found to complicate flight maneuvers [8].

The investigation into how twist at the tip can affect the noise production is limited, but has had some results that would suggest further work into this could have some good results [9]. The interest in how twist can affect the production of the BVI noise is due to the lower tip speeds associated with smaller rotor blades for the use in air taxis than in traditional helicopters. It was determined that the rotor wake and blade tip vortex strengths have an effect on the generation of BVI noise [11]. The focus of this study is on the affects blade tip twist has on the acoustic signature through analyzing the contour plots of the overall sound pressure levels experienced by fix observer points.

III. Methodology

A. Modeling Code

The modeling program used for this study was a high-fidelity aeromechanics modeling computer program developed by Continuum Dynamics Inc. The modeling program is called the Comprehensive

Hierarchical Aeroacoustics Rotorcraft Model also known as CHARM. The CHARM code was used to model the aeromechanics of vertical take-off and landing (VTOL) aircraft in steady flight [14]. The CHARM code has the capabilities to accurately generate predictions of the aircraft's vibrations, wake geometry, aerodynamics, performance, and structural loads [14]. This modeling program was coupled with an aeroacoustic prediction code called PSU-WOPWOP which was developed by Pennsylvania State University based from NASA's WOPWOP prediction code. The CHARM code is automatically coupled with PSU-WOPWOP to generate the sound pressure level output files, the dBA output files, the wake geometry files along with many others such as frequency files to aid in understanding the acoustic effects of the rotor [14].

The set up for this study had the CHARM program installed in a Linux environment. The user input files were edited directly within a command shell. The CHARM generated output files were processed using utility programs provided in CHARM. The CHARM output files were processed in PSU-WOPWOP prediction code to generate the overall sound pressure values in dBA. The overall sound pressure level in dBA (OASPLdBA) data was plotted in contour plots for all trials. The delta values between the nominal trial, Trial z0, and consequent trials were also plotted to evaluate the overall effects each change to the blade tip twist had on sound pressure levels experienced by an observer point.

The study design used an airfoil symmetric about the camber line and has a maximum thickness of 12% for the rotor blade. This airfoil was the NACA 0012 airfoil. The characteristics of the rotor blade can be found in Table 1.

B. Rotor Blade Characteristics

The airfoil used for this study is the NACA 0012. This airfoil is symmetrical with maximum thickness of 12% located at 30% of the chord length. The rotor has two blades with an 8-foot radius and chord length of 1.719 feet.

Airfoil	Number of Blades	Chord	Blade Radius	Taper	Solidity	Tip Speed
NACA 0012	2	1.719ft	8 ft	0.25	0.113	720 ft/s

Table 1: Characteristics of the rotor blade

C. Observer Points

The CHARM code coupled with PSU-WOPWOP acoustic prediction code generates the thickness and loading noise data at specified observer points [14]. The coordinate plane is set up where the +X direction is the advancing direction of the blade, the +Y direction is to the right of the advancing direction, and +Z direction is the direction of the inflow [14]. At the +X axis is where the azimuth angle value is 90 degrees and the +Y axis is at zero azimuth angle [14]. The location of these observer points span azimuth angles ranging from 40 degrees to -80 degrees on the X-Y coordinate plane and an elevation angle range of 0 degrees to 70 degrees in the +Z direction [14]. There are a total of 25 observer points that enclose almost a quadrant of a hemisphere. The observer points are fixed relative to the rotor at a radius of 15m or 50ft from the center of the rotor and are equally distributed in a spherical formation with an observer point located directly below the center of the rotor shaft [14]. See Figure 2 for the distribution of the observer points.

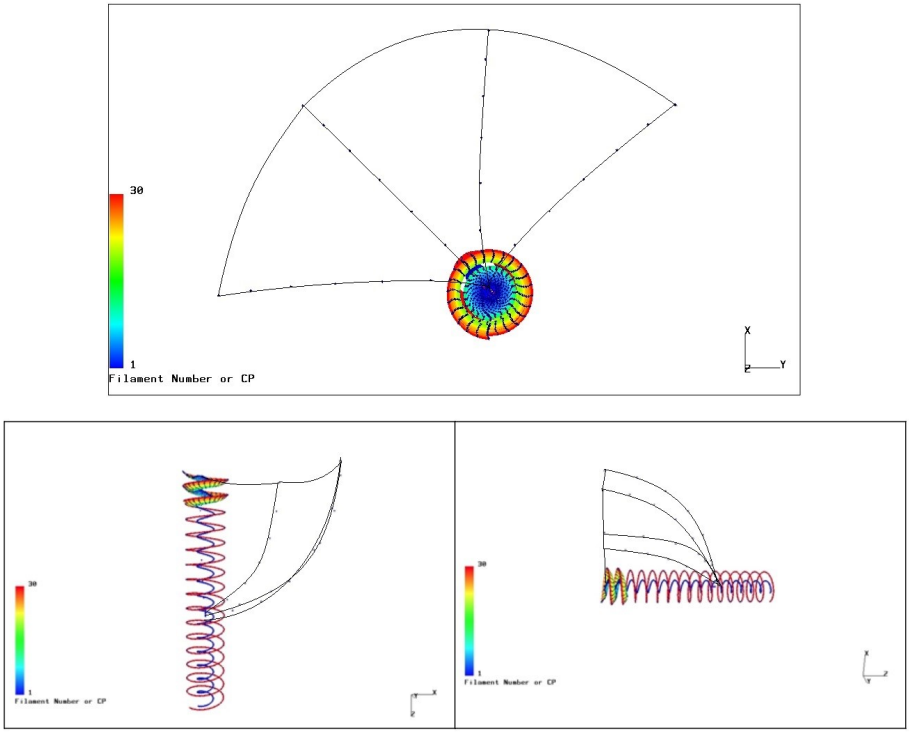

Fig. 2: Top and side views of the azimuth observer points locations spanning from $40deg$ **to** $-80deg$**.**

D. Trials

In order to apply changes to the twist, the rotor blade was divided into 12 segments that were equidistant from one another starting from the tip of the blade to 80% of the blade span. Any change made to the twist of the rotor blade went through linear interpolation between each segment. The preliminary trials tabulated in Table 2 varied the rotational speed and the twist that explored vortex formation at the blade tip. The flow fields of these trials were captured through a built-in executable graphics code in CHARM. The second set of trials tabulated in Table 3 explored effects of varied twist on the overall sound pressure levels. The initial conditions for

this trial were set at a constant root twist of 20 degrees and a constant rotational speed of $\Omega = 90\ rad/s$. The third set of trials charted in Table 4 examined the overall sound pressure levels at a constant root twist of 45 degrees and a constant rotational speed of $\Omega = 90\ rad/s$. The last set of trials in Table 5 and 6 took Trial 5 and 6 of the third set of trials with the same initial conditions and varied the rotational speed. The use of Trials 5 and 6 for varied Ω values were chosen arbitrarily.

Trial	Twist (deg)	$\Omega(rad/s)$
1	-10.97	90
2	-20.97.	120
3	-20.97	34
4	-20.97	24
5	-20.97	90
6	-46.02	90
7	-49.35	90

Table 2: Preliminary trials with varied twist and Ω

The twist was plotted against the radius in Fig. 3 and Fig. 4 for trial sets one and two. The trails investigated twist in both the positive and negative direction and kept the rotational speed at a constant.

Trial	Twist (*deg*)	Ω(*rad/s*)
z0	-17.632	90
z1	-22.52	90
z2	-10.513	90
z3	-18.513	90
z4	-26.513	90
z5	5.933	90
z6	13.933	90
z7	21.93	90

Table 3: Trial Set 1 - Initial Root Twist set at 20 degrees and Ω= 90*rad/s*

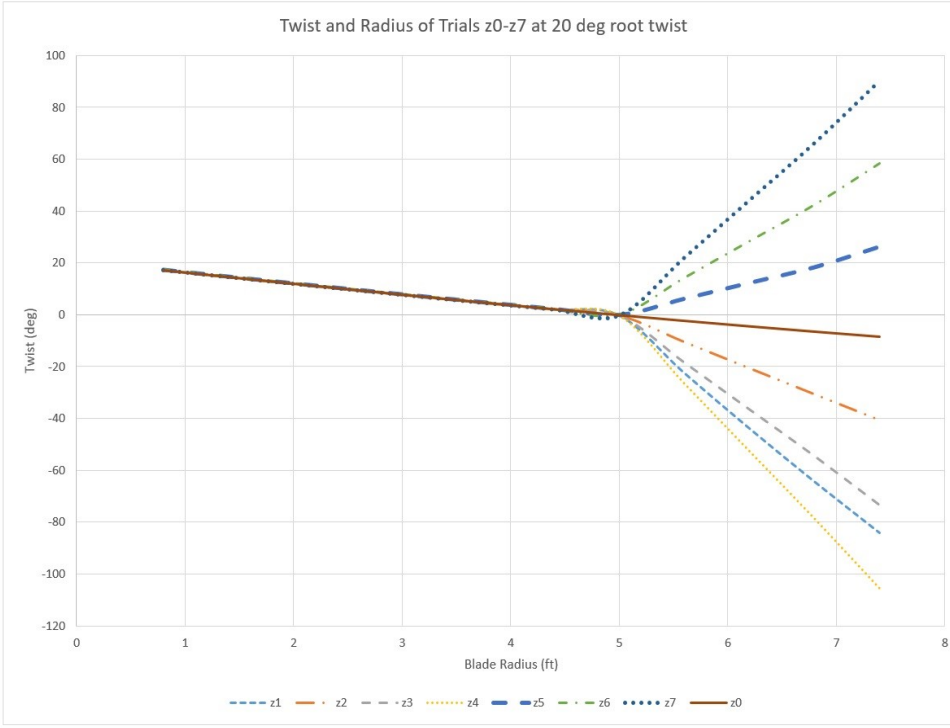

Fig. 3: Comparisons of the Twist and Radius of all trials with 20 *degree* root twist.

Trial	Twist (*deg*)	$\Omega(rad/s)$
z0	-22.368	90
z1	-42.375	90
z2	-30.368	90
z3	-38.368	90
z4	-43.632	90
z5	13.922	90
z6	21.922	90
z7	29.078	90

Table 4: Trial Set 2 - Initial Root Twist set at 45 degrees and constant $\Omega = 90 rad/s$

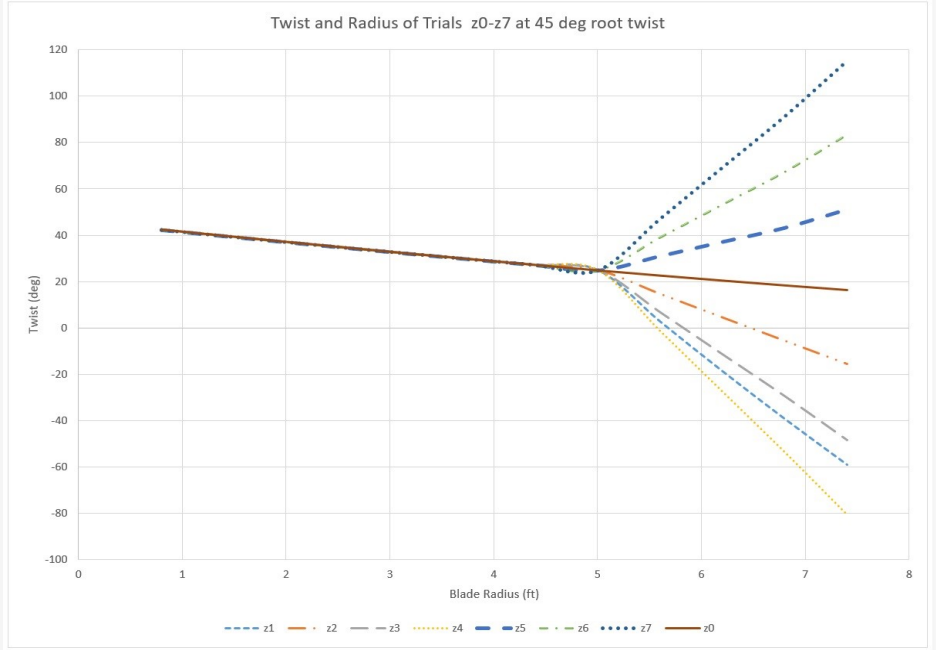

Fig. 4: Comparisons of the Twist and Radius of all trials with 45 *degree* root twist.

Trial	Twist (*deg*)	Ω(*rad*/*s*)
z5	13.922	70
z5	13.922	80
z5	13.922	90
z5	13.922	100
z5	13.922	110
z5	13.922	120
z5	13.922	130
z5	13.922	140
z5	13.922	150

Table 5: Trail Set 3 - Trial z5 at initial 45 degrees root twist and varied Ω values

Trial	Twist (*deg*)	Ω(*rad*/*s*)
z6	21.922	70
z6	21.922	80
z6	21.922	90
z6	21.922	100
z6	21.922	110
z6	21.922	120
z6	21.922	130
z6	21.922	140
z6	21.922	150

Table 6: Trial Set 4 - Trial z6 at initial 45 degrees root twist and varied Ω values

IV. Results

Results from the trials were processed and visualized via flow fields and contour plots. The preliminary trials explored the change in pressure of the blade vortex generated at the tip. This is visualized through flow fields shown in Fig. 8. Flow fields aid in understanding the pressure distribution and flow interaction in the wake of the rotor blades. Trial 2 in Fig. 8 displays a side view of the flow field. Each filament has a distinct pressure from the next. The concentration of filaments and high pressure indicated by the color gradient along the edge of the helix-shaped flow field indicated a strong blade tip vortex. The flow fields corresponding to the trials 2 to 5 showed as rotational speed increased, the pressure of each filament increased and clustering occurred towards the outer edge of the flow. The filaments in trial 2 towards the edge were more spaced out than that of trial 5, but the overall shape of the flow in the top view indicate some downwash may have occurred. The increase in RPM also increased in the intensity of the blade vortex at the tip.

The results from Trial Sets 2-4 were analyzed through contour plots. The plots for Trial Set 2 showed increase in noise production as observer points approached the in-plane of the rotor blade. The contour plot Trial z0-z2 showed a slight increase of 1 dBA in noise at observer point where Θ is 70deg and Φ is at 40deg when the twist went from -22.368 deg to -30.386 deg. The plots for Trial z0-z4, z0-z1, and z0-z3 exhibit an increase in noise production as the twist approached -45 degree twist. The noise production also increased in positive twist configurations. The contour plot for Trial z0-z5 through z0-z7 also displayed increase in noise experienced by the observer points. The noise increased at a higher rate at positive twist than at negative twist.

The contour plots of Trial Set 3 conveyed the effect of rotational speed on noise production. At rotational speed set at Ω= 70 rad/s, the contour plot demonstrated fluctuating noise levels detected by the observer points. As the omega increased, contours began to reach a uniform shape between each observer point. At Ω= 100 rad/s, the noise increase experienced by the observer increased incrementally by 10 dBA with each increase to omega by 10 rad/s up to Ω= 130 rad/s. At Ω= 140 rad/s, the contour plots showed significant increase in not only the blade-vortex interaction noise, but also the loading and broadband noise. From

140rad/s to 150 rad/s, the observer points at Θ= 10 across Φ values experienced 200 dBA compared to 75 to 80 dBA. As the rotational speed increased, the contour plots exhibited a shift in the formation of BVI noise in a direction towards the rotor plane.In Trail Set 4, the contour plot for Ω= 100 rad/s depicted a small pocket of noise which was inconsistent with the rest of the plots. An assumption was the observer point experienced a small blade wake interaction.

From the results, the noise produced by the rotor blade increased as the rotational speed increased. There was a shift in the concentration of the BVI noise as the rotational speed increased as well. Higher blade speed also meant there was more turbulence at the wake of the rotor and as a result, higher broadband noise was experienced at the observer points directly below the rotor.

A. Flow Fields

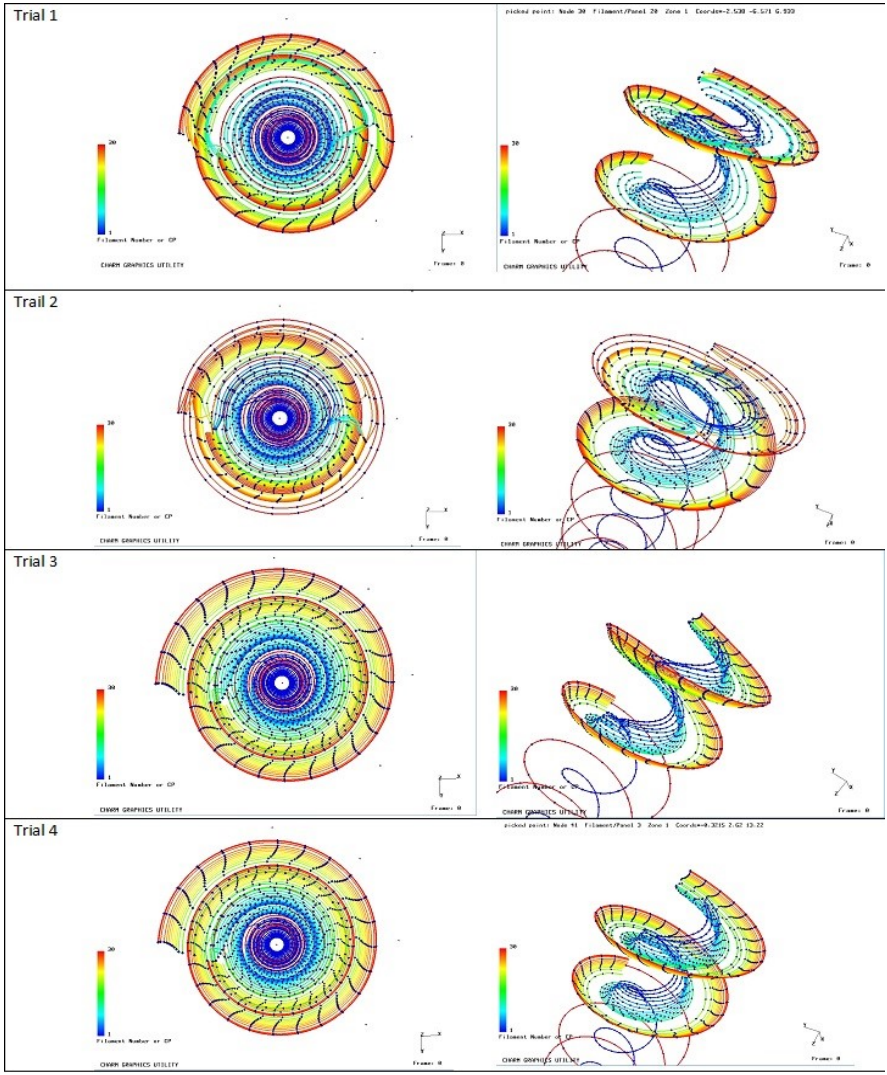

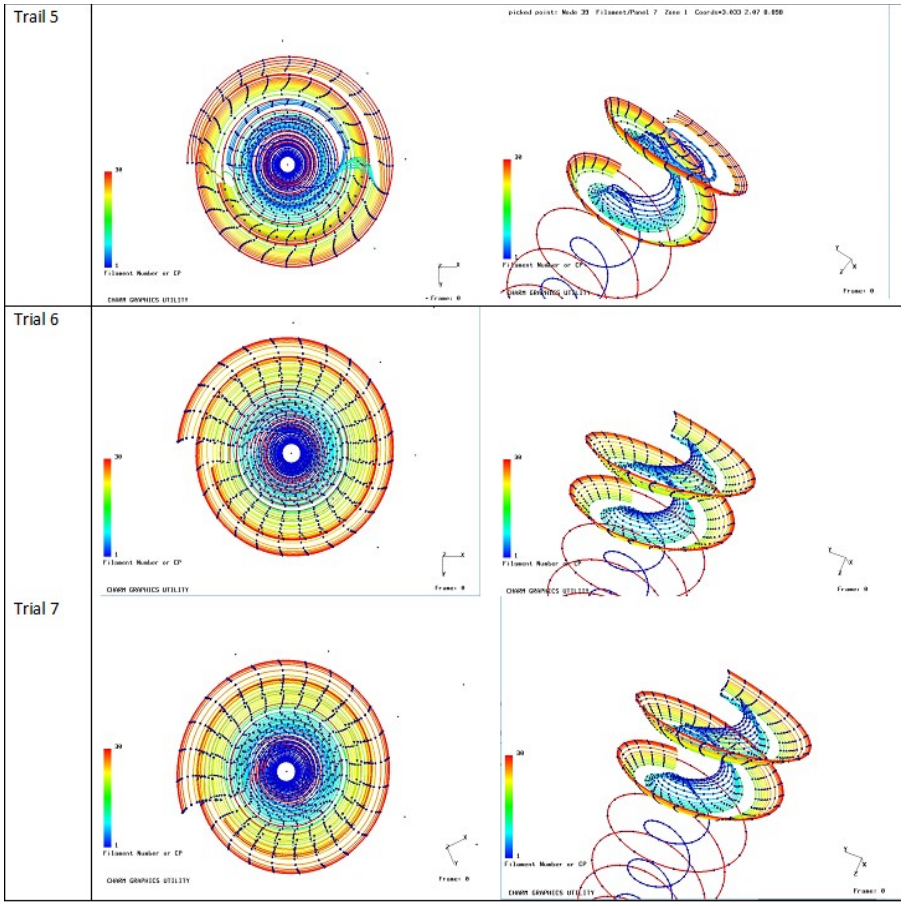

Fig. 8: Top and isometric view of flow fields of preliminary trials 1-7 showing pressure and filament distribution

B. Contour Plots

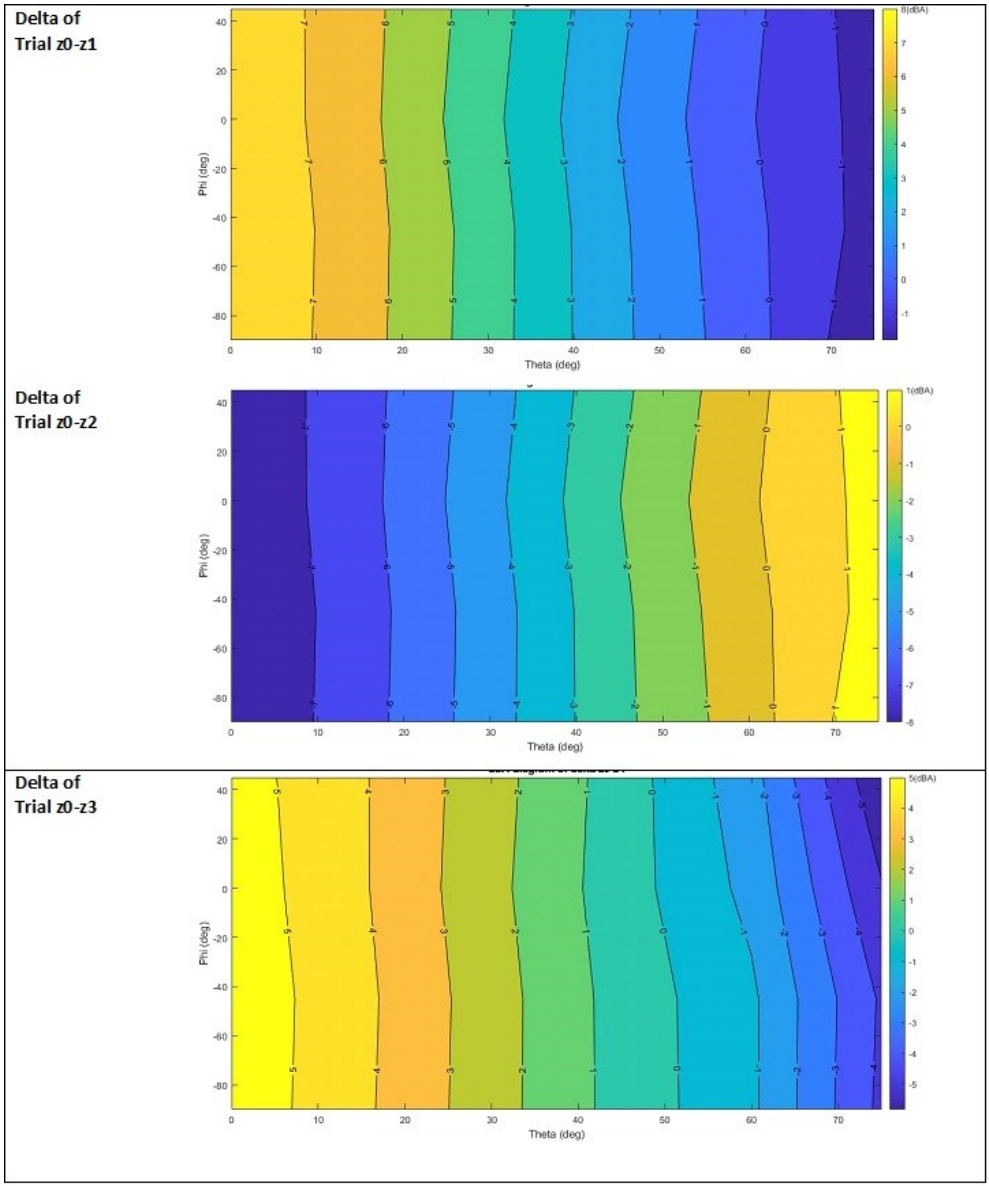

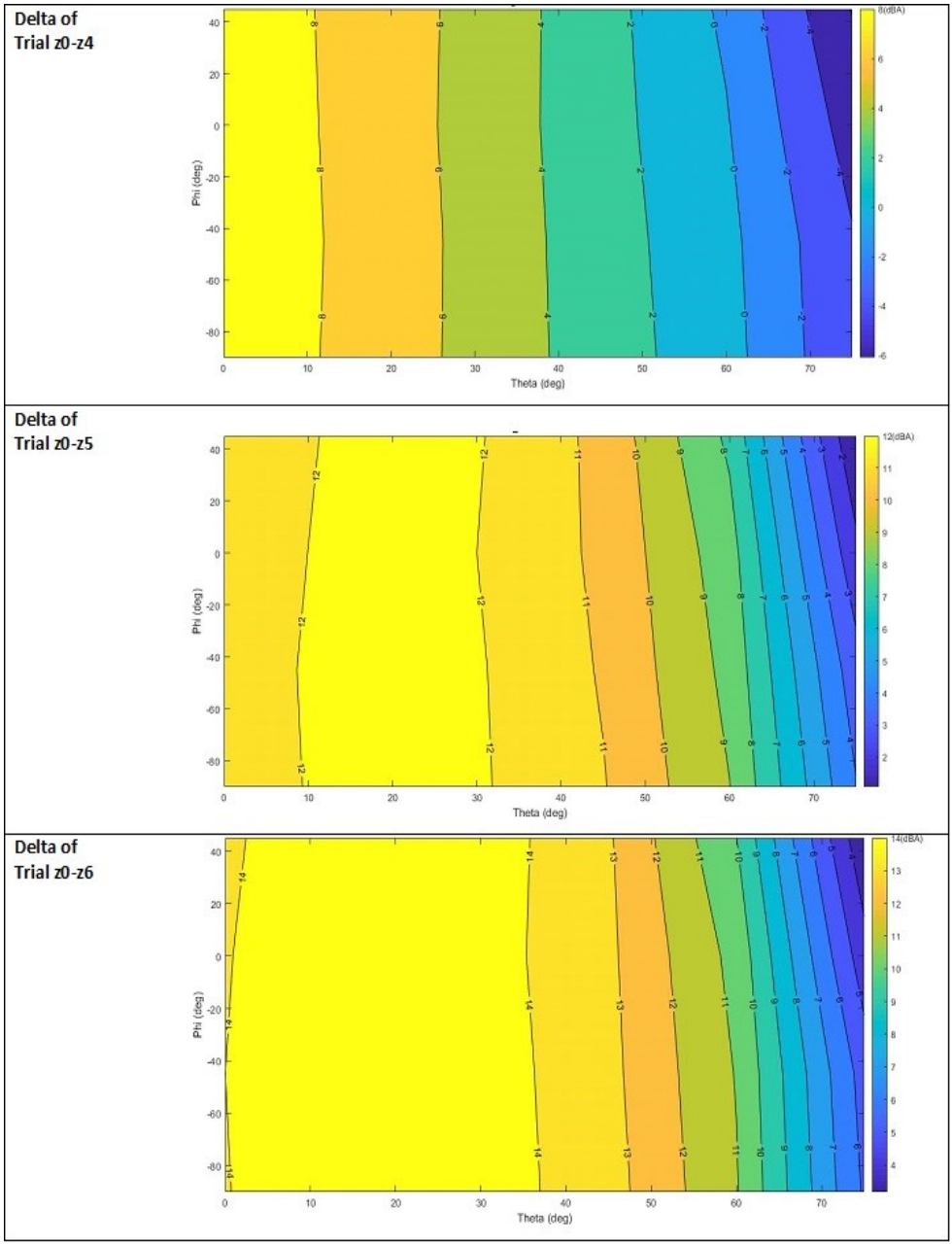
Delta of
Trial z0-z4
8(dBA)
Phi (deg)
Theta (deg)
Delta of
Trial z0-z5
12(dBA)
Phi (deg)
Theta (deg)
Delta of
Trial z0-z6
14(dBA)
Phi (deg)
Theta (deg)

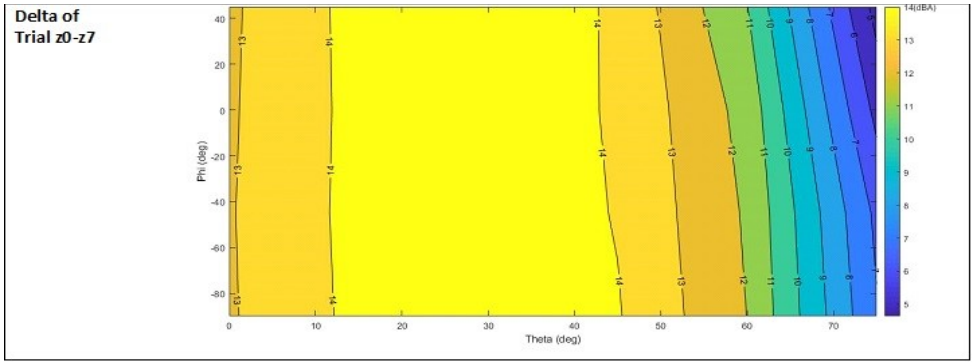

Fig. 5: Trial Set 2 - contour plots showing the sound pressure levels at each observer point

Trial z0-z5 at 70 rad/s	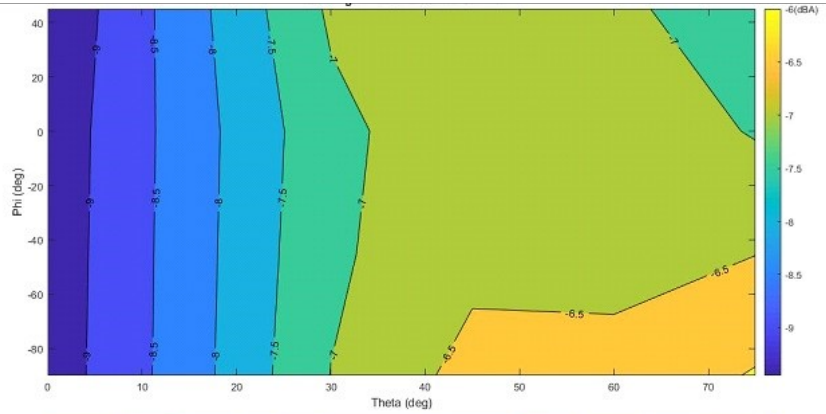
Trial z0-z5 at 80 rad/s	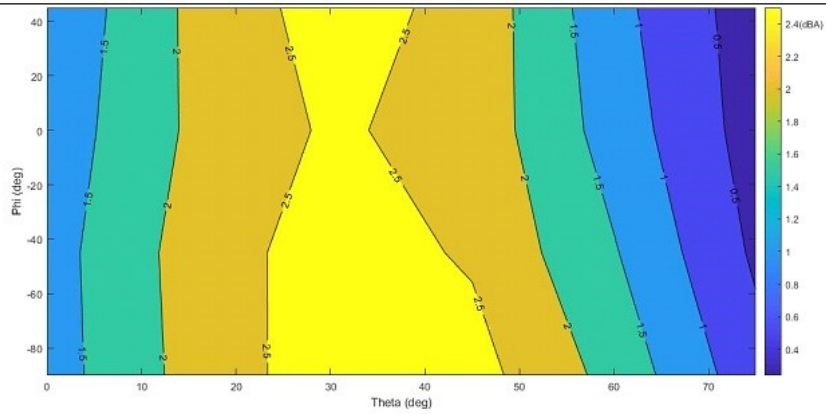

Trial z0-z5 at 90 rad/s	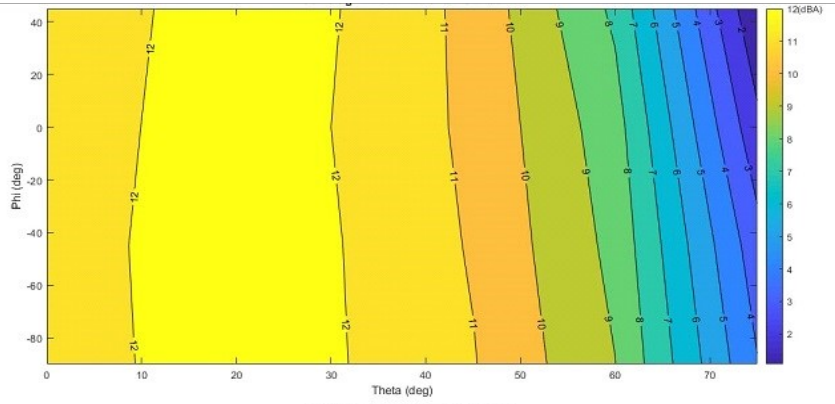
Trial z0-z5 at 100 rad/s	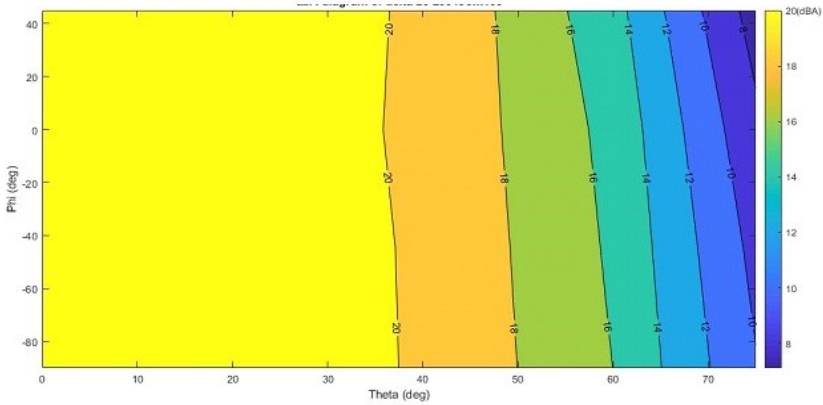

Trial z0-z5 at 110 rad/s	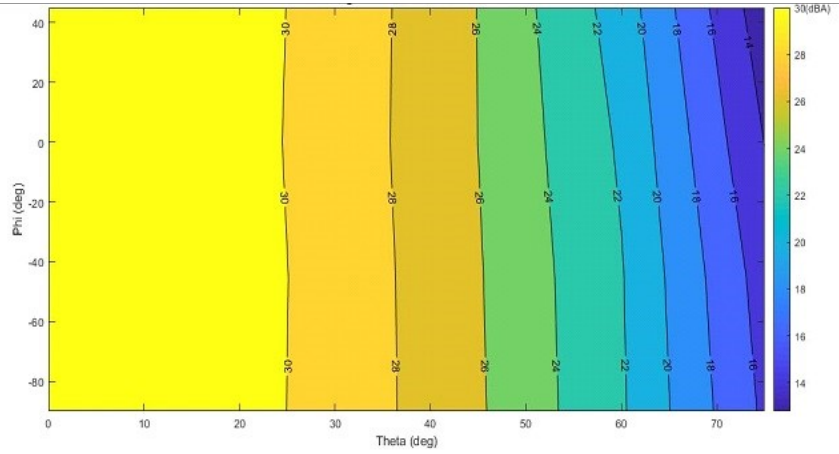
Trial z0-z5 at 120 rad/s	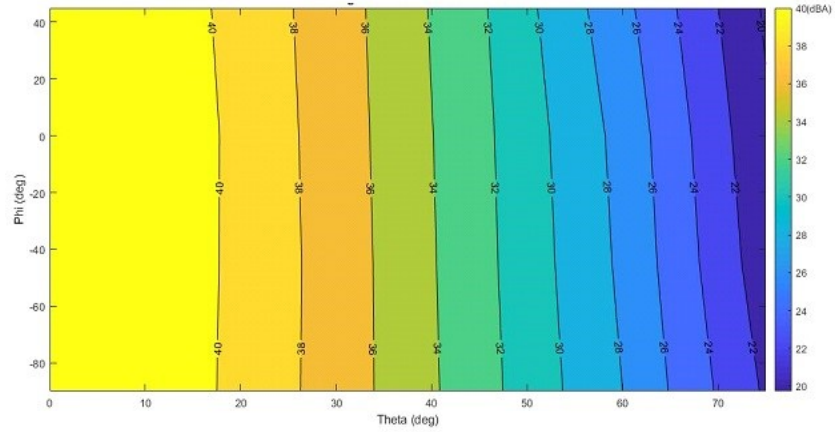

Trial z0-z5 at 130 rad/s	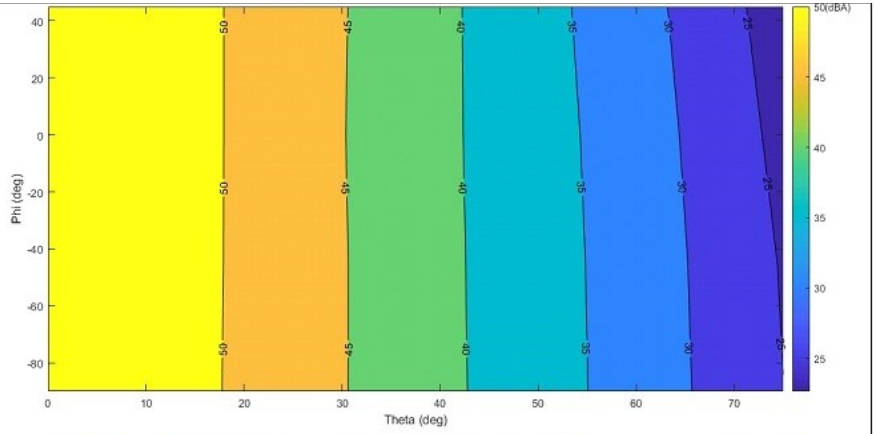
Trial z0-z5 at 140 rad/s	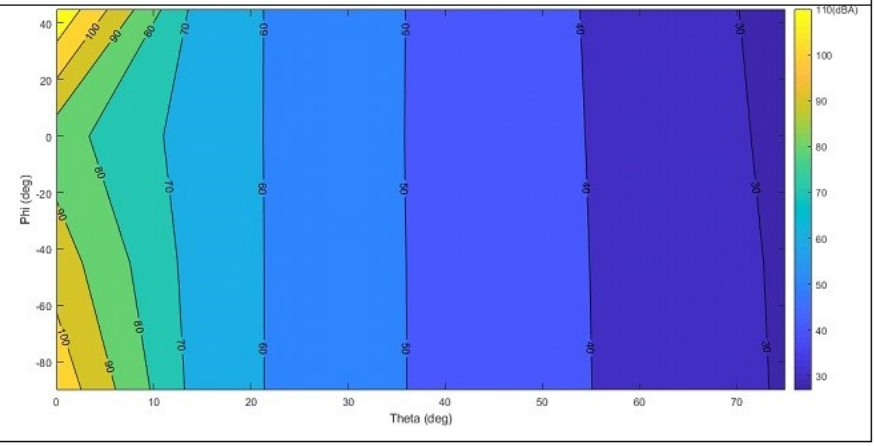

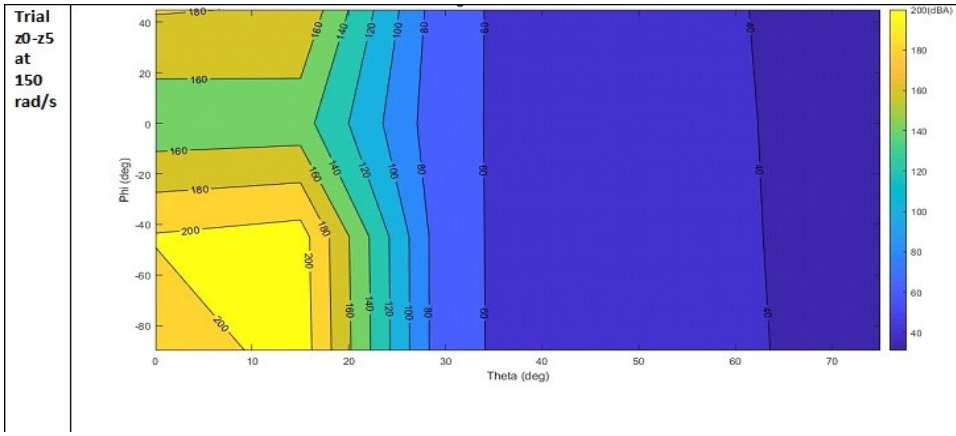

Fig. 6: Trial Set 3 - contour plots showing the sound pressure levels at each observer point

Trial z0-z6 at 70 rad/s	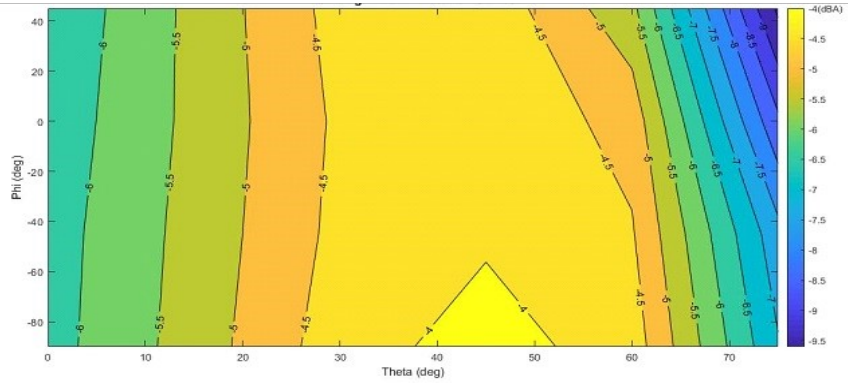
Trial z0-z6 at 80 rad/s	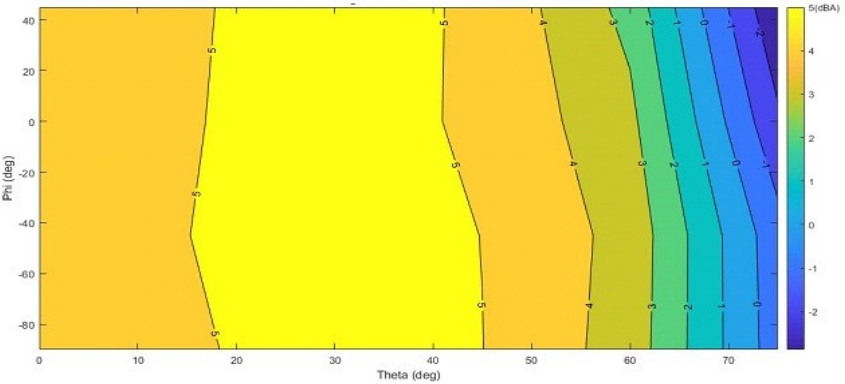

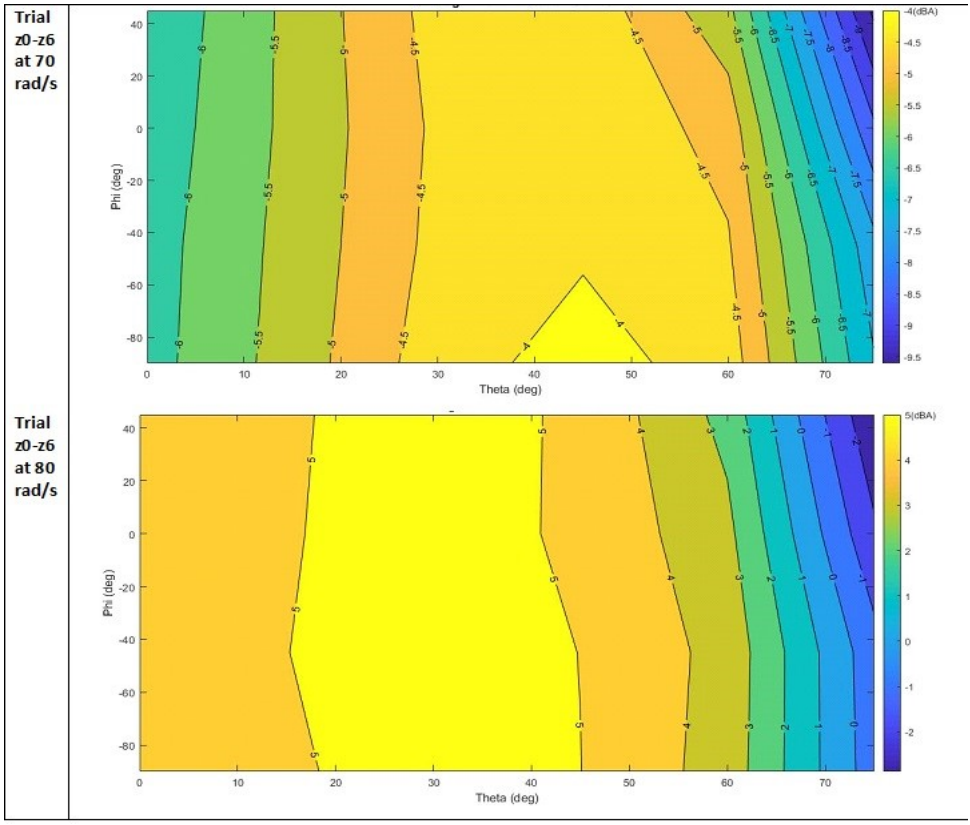
Trial z0-z6 at 70 rad/s
Phi (deg)
Theta (deg)
-4(dBA)
Trial z0-z6 at 80 rad/s
Phi (deg)
Theta (deg)
5(dBA)

Trial z0-z6 at 70 rad/s	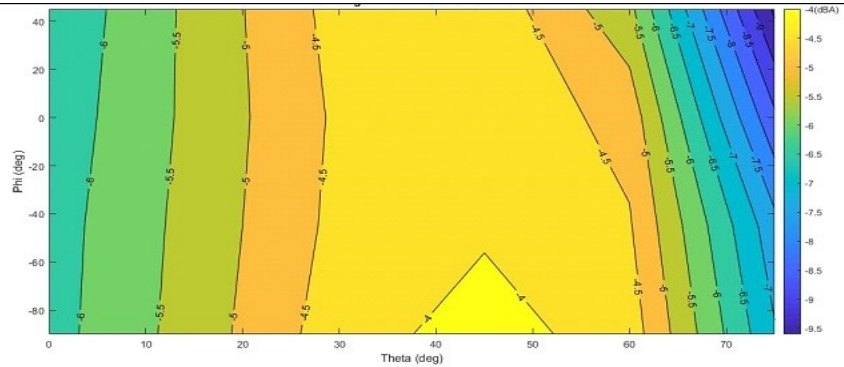
Trial z0-z6 at 80 rad/s	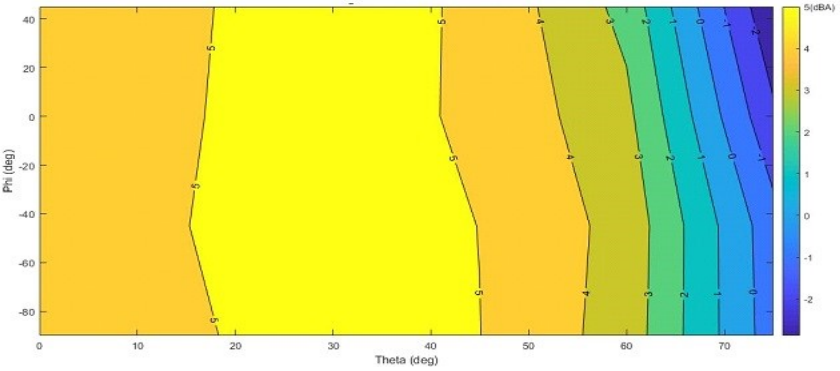

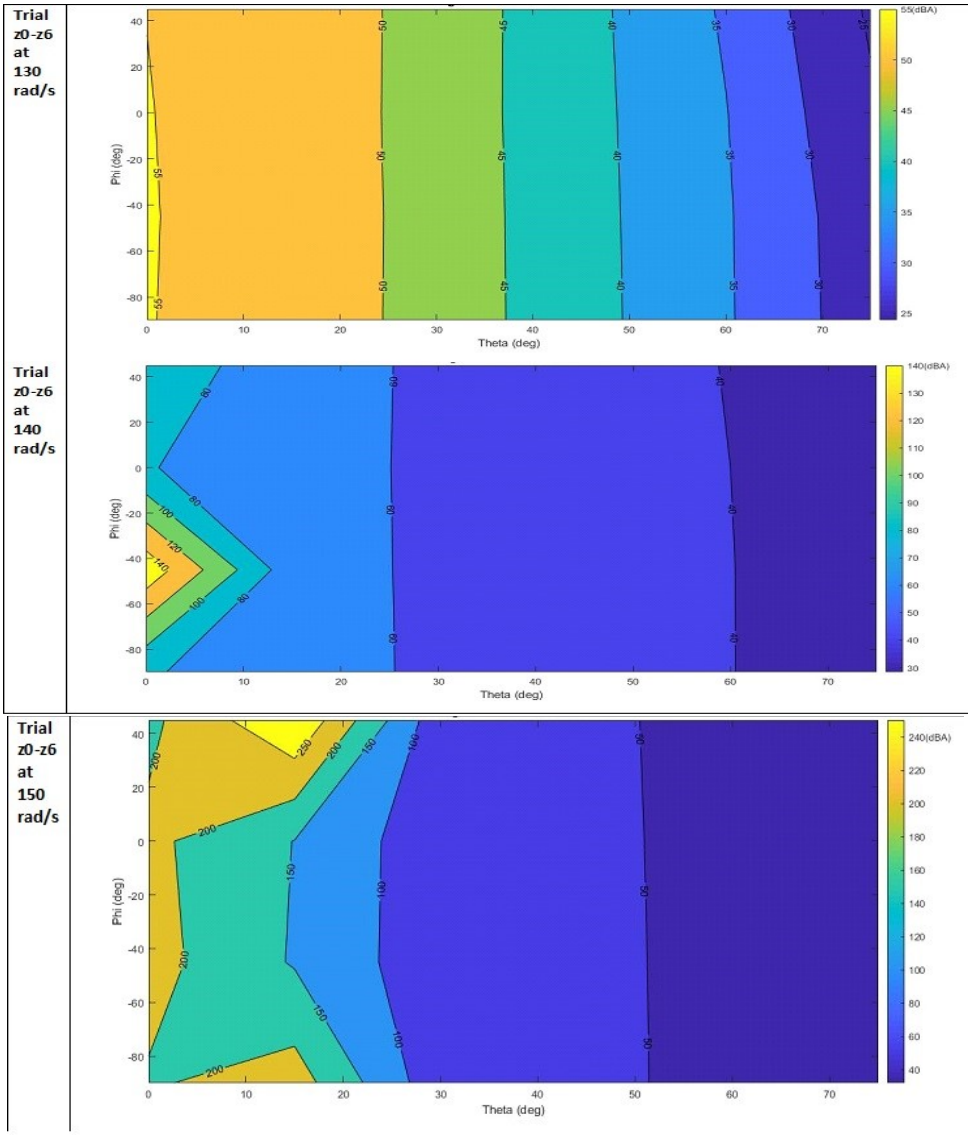

Fig. 7: Trial Set 4 - contour plots showing the sound pressure levels at each observer point

V. Conclusion

The balance between rotorcraft performance and its acoustic signature is a key hurdle the Urban Air Mobility (UAM) community must overcome. Aircraft designers can design a rotor that meets the noise restrictions by addressing a major source of the noise. Blade-vortex interaction noise is a major concern due to humans' perception of the noise. Humans consider BVI noise to be highly annoying and since public acceptance is vital to UAM success focus on reducing this noise is important. Adjusting the twist at the blade tip is a method to reducing the BVI noise because blade tip twist affects the formation of vortices in the following ways. Blade tip twist affects the intensity and the formation location of tip vortices. The results suggested that the intensity of sound pressure level observed at fixed observer points appeared to shift towards the direction of the rotor plane. The blade tip twist seems to influence the position and concentration of blade vortex interaction noise experienced by the observer points below the rotorcraft. Future work would be to investigate whether blade tip twist could be used as a method to affect position of vortex formation to increase the miss distance between the advancing blade and the tip vortex.

VI. Acknowledgements

The author would like to thank Dr. Nicholas B. Cramer, Dr. Sean Swei, and Dr. Maria E. Cruz, for all their guidance and support. The author would also like to thank Taylor-Dawn Francis for her help as well. This would not be possible without the Ronald E. McNair Scholars Program at San José State University.

References

[1] Zawodny, N. S., Boyd Jr., D. D., and Burley, C. L., "Acoustic Characterization and Prediction of Representative, Small-Scale Rotor-Wing Unmanned Aircraft System Components," *NASA Technical Report Server*, 2018.

[2] Pascioni, K. A., and Rizzi, S. A., "Tonal Noise Prediction of a Distributed Propulsion Unmanned Aerial Vehicle," *AIAA AVIATION Forum: AIAA/CEAS Aeroacoustics Conference*, Atlanta, GA, 2018.

[3] Wachspress, D. A., and Quackenbush, T. R., "BVI Noise Prediction using a Comprehensive Rotorcraft Analysis," *American Helicopter Society 57th Annual Forum*, Washington, DC, 2001.

[4] Horn, J. F., Bridges, D. O., Wachspress, D. A., and Rani, S. L., "Implementation of a Free-Vortex Wake Model in Real-Time Simulation of Rotorcraft," *AIAA Journal of Computing, Information, and Communications*, Vol. 3, No. 3, 2006.

[5] Brooks, T. F., and Burley, C., "Blade Wake Interaction Noise for a Main Rotor," *AHS Technical Specialists' Meeting for Rotorcraft Acoustics and Aerodynamics*, 2004, pp. 11–27.

[6] Cabell, R., McSwain, R., and Grosveld, F., "Measured Noise from Small Unmanned Aerial Vehicles," *Noise-CON*, Providence, RI, 2016.

[7] Yu, Y. H., "Rotor blade-vortex interaction noise," *Environmental Health Perspectives*, Vol. 36, 2000, pp. 95–115.

[8] Brooks, T. F., Jolly Jr., J. R., and Marcolini, M. A., "Helicopter Main Rotor Noise: Determination of Source Contributions Using Scaled Model Data," Tech. rep., NASA Scientific and Technical Information Division, 1988.

[9] Shi, Y., Li, T., He, X., Dong, L., and Xu, G., "Helicopter Rotor Thickness Noise Control Using Unsteady Force Excitation," *Applied Sciences*, Vol. 9, No. 1351, 2019, pp. 1–17.

[10] Malovrh, B. D., "Non-Harmonic Root-Pitch Individual-Blade Control for the Reduction of Blade-Vortex Interaction Noise in Rotorcraft," Ph.D. thesis, Pennsylvania State University, 2012.

[11] Brentner, K. S., and Farassat, F., "Modeling aerodynamically generated sound of helicopter rotors," *Progress in Aerospace Science*, 2018.

[12] Landgrebe, A. J., and Bellinger, E. D., "Experimental investigation of model variable geometry and ogee tip rotors," *NASA Technical Report*, Vol. CR-2275, 1974.

[13] Brocklehurst, A., and Barakos, G. N., "A review of helicopter rotor blade tip shapes," *Progress in Aerospace Science*, Vol. 56, 2012, pp. 35–74.

[14] Wachspress, D. A., Quackenbush, T. R., Boschitsch, A. H., Yu, M. K., and R, W. G., *CHARM User's Manual (Comprehensive*

Hierarchical Aeromechanics Rotorcraft Model), Continuum Dynamics Inc., 34 Lexington Ave., Ewing, NJ 08618-2302, version 6.4 ed., May 2018. 18-06.